Sci Immunol. Author manuscript; available in PMC 2017 June 28.

Published in final edited form as:

Sci Immunol. 2016 September 02; 1(3): . doi:10.1126/sciimmunol.aaf8864.

The orphan nuclear receptor ROR alpha and group 3 innate lymphoid cells drive fibrosis in a mouse model of Crohn's disease

Bernard C. Lo[1], **Matthew J. Gold**[1], **Michael R. Hughes**[1], **Frann Antignano**[1], **Yanet Valdez**[2], **Colby Zaph**[1,3], **Kenneth W. Harder**[4], and **Kelly M. McNagny**[1,*]

[1]The Biomedical Research Centre, University of British Columbia, V6T 1Z3

[2]STEMCELL Technologies Incorporated, Vancouver, British Columbia, V6A 1B6

[3]Infection and Immunity Program, Monash Biomedicine Discovery Institute, Monash University, Clayton, VIC, 3800, Australia

[4]Department of Microbiology and Immunology, University of British Columbia, Vancouver, British Columbia, V6T 1Z3

Abstract

Fibrosis is the result of dysregulated tissue regeneration and is characterized by excessive accumulation of matrix proteins that become detrimental to tissue function. In Crohn's disease, this manifests itself as recurrent gastrointestinal strictures for which there is no effective therapy beyond surgical intervention. Using a model of infection-induced chronic gut inflammation, we show that *Rora*-deficient mice are protected from fibrosis; infected intestinal tissues display diminished pathology, attenuated collagen deposition and reduced fibroblast accumulation. Although *Rora* is best known for its role in ILC2 development, we find that *Salmonella*-induced fibrosis is independent of eosinophils, STAT6 signaling and Th2 cytokine production arguing that this process is largely ILC2-independent. Instead, we observe reduced levels of ILC3- and T cell-derived IL-17A and IL-22 in infected gut tissues. Furthermore, using $Rora^{sg/sg}/Rag1^{-/-}$ bone marrow chimeric mice, we show that restoring ILC function is sufficient to re-establish IL-17A and IL-22 production and a profibrotic phenotype. Our results show that RORα-dependent ILC3 functions are pivotal in mediating gut fibrosis and they offer an avenue for therapeutic intervention in Crohn's-like diseases.

Introduction

Fibrosis is the pathological deposition of extra-cellular matrix (ECM) associated with persistent inflammation. The contribution of the hematopoietic system to this process has

*Corresponding author: Kelly M. McNagny, The Biomedical Research Centre, 2222 Health Sciences Mall, Vancouver, BC, V6T 1Z3, kelly@brc.ubc.ca.

Author contributions: B.C.L., M.J.G., M.R.H., F.A., performed experiments; B.C.L., M.J.G., M.R.H., F.A., K.M.M, designed the experiments and analyzed data, C.Z. and K.W.H. provided reagents; M.J.G., Y.V., C.Z., K.W.H contributed to manuscript preparation; B.C.L. and K.M.M. wrote the manuscript.

Competing interests: The authors declare no competing financial interests.

been widely investigated and numerous leukocyte subsets are implicated in driving fibrotic remodeling including M2 macrophages, neutrophils, eosinophils, mast cells and lymphocytes (1, 2). In particular, type 2 immune responses have long been associated with tissue fibrosis and IL-4 and IL-13 signaling has been shown to drive tissue remodeling and ECM deposition in the liver in response to *Schistosoma mansoni* infection (3). In mucosal tissues both $CD4^+$ T helper 2 (Th2) and Th17 cells have been linked to the development of tissue fibrosis. For example, in a mouse model of chronic gut inflammation and fibrosis, an overlapping production of IL-13 and IL-17A coincides with the appearance of fibrotic tissue, which suggests the pathology may be driven by a mixed Th2 and Th17 response (4).

Innate lymphoid cells (ILCs) are a recently identified subset of leukocytes and a prominent source of cytokines with profiles similar to those of T helper cells, yet these cells lack antigen-specific receptors and their temporal production of cytokines precedes adaptive immune responses. ILCs can be classified based on their transcript and cytokine profiles; for instance, group 2 ILCs (ILC2s) are GATA3- and RORα-dependent and produce IL-5 and IL-13 while group 3 ILCs (ILC3s) express RORγt and are a source of IL-17A and IL-22. ILCs have broad functions in host defense responses against pathogens, maintenance of tissue homeostasis, and pathologies such as allergic asthma and colitis (5). Recently, ILC2s were shown to have the capacity to drive excessive lung collagen deposition; likewise, analyses of idiopathic pulmonary fibrosis patient bronchoalveolar lavage fluid (BAL) revealed an expansion of ILC2s, providing correlative evidence that ILCs may be pathogenic in fibrotic remodeling (6). Despite their pathogenic role in these models, ILC2s have also been shown to play a critical role in tissue repair. For example, in mouse models of lung influenza infection (7) and DSS-induced colitis (8) ILC2s aid tissue repair through their production of amphiregulin.

Similarly, ILC3s in the gut demonstrate protective or pathogenic roles depending on context. ILC3s are necessary for pathogen clearance (9, 10) and gut tissue repair following chemotherapy-induced injury. This is likely through IL-22-dependent activation of epithelial progenitors (11), but ILC3s can also promote intestinal tumor formation in a chronic inflammatory setting (12). In summary, there are data to support both beneficial and pathogenic roles for ILC2s and ILC3s in tissue remodeling.

Crohn's disease (CD) is primarily characterized as a Th17-driven disease (13), and distinct IL-23-dependent ILCs that produce IL-17A and IL-22 are also elevated in CD patient samples (14, 15) arguing for a role for Th17 cytokines. Conversely, other studies have suggested that ILC2s and eosinophils are contributing factors to CD progression through an IL-13 dependent accumulation of matrix-producing fibroblasts (16, 17). Thus, there is evidence to support both Th2 and Th17 responses in the pathology of CD. However, the direct involvement of ILCs in driving excessive tissue remodeling and ultimately fibrosis in the gut remains unclear.

RORα is a transcription factor known to regulate ILC2 development. It is closely related to RORγt, which is a critical regulator of Th17 and ILC3 subsets including lymphoid tissue-inducer cells (18–20). Moreover, in the Th17 lineage, RORγt and RORα are co-expressed and function synergistically for lineage maintenance and cytokine production (21).

Previously we showed that *Rora*$^{sg/sg}$ bone marrow transplant (BMT) chimeric mice provide a suitable model of ILC2 deficiency as they selectively lack ILC2s while other leukocyte lineages, including other ILCs, are present at steady state (22). Furthermore, *Rora*$^{sg/sg}$ BMT animals are protected from type 2 immune lung pathology (22–24). In this report, we used a similar strategy to evaluate their role in a *Salmonella*-induced model of gut fibrosis. Strikingly, we show that RORα is required for a fibrotic response. Surprisingly, this is not through regulation of ILC2-dependent production of type 2 cytokines, but rather through a previously unrecognized role for RORα in the production of cytokines from ILC3s. We also find that restoration of ILCs in *Rora*$^{sg/sg}$ BMT mice is sufficient to reestablish susceptibility to fibrotic disease. These data provide evidence that ILC3s contribute to fibrosis, and offer RORα as a new therapeutic target for fibrotic tissue remodelling.

Results

Salmonella-induced gut pathology is dependent on hematopoietic expression of RORα

We generated *Rora*$^{sg/sg}$ BMT mice and evaluated how they respond to infection with the Δ*aroA* strain of *Salmonella* Typhimurium, which induces robust ECM deposition in the cecum (25). We find no differences in pathogen burdens in the ceca or spleens of WT BMT and *Rora*$^{sg/sg}$ BMT mice at days 7, 21, and 35 postinfection (pi), indicating that *Rora* is dispensable for *Salmonella* clearance (Fig. 1A). In addition, we find similar degrees of mucosal thickening, edema, and inflammatory infiltrates in these animals at day 7 pi (Fig. 1B). In contrast, at 21 days pi, during peak fibrosis, we observe pronounced epithelial cell hyperplasia and pathological remodeling of normal tissue architecture, including disruption and thickening of the basal lamina in WT BMT ceca, whereas we find a striking attenuation in collagen deposition and dampened immunopathology in cecal sections of *Rora*$^{sg/sg}$ BMT mice. Similarly, by day 35 pi, much of the pathology and inflammation is resolved in *Rora*$^{sg/sg}$ BMT mice, with mucosa thickness returning to levels similar to uninfected samples (albeit with some residual collagen in the submucosal regions) (Fig. 1B). Conversely, WT BMT cecal sections reveal persistent tissue inflammation and lymphoid cell aggregates at this time point (Fig. 1B, C).

In evaluating cytokine production, we find *Tnfa* and *Il6* transcripts are present at similar levels at day 7 pi, but are significantly reduced in *Rora*$^{sg/sg}$ BMT cecal samples at the day 21 and 35 time points (Fig. 1D). Consistent with these mRNA results, quantification of cytokines in cecal homogenates reveals significantly less TNF, IL-6, MCP-1, and IL-10 (but comparable levels of IL-12p70 and IFN-γ) in *Rora*$^{sg/sg}$ BMT samples when compared with their WT BMT counterparts at day 21 pi (Fig. 1E). In summary we find that deletion of *Rora* leads to attenuated inflammatory responses associated with fibrosis and these correlate with a more rapid resolution of immunopathology and tissue architecture during the late phases of chronic *Salmonella* infection.

Fibrosis is attenuated in *Rora*$^{sg/sg}$ BMT mice during chronic infection

Consistent with a role for RORα in driving fibrosis we find significantly reduced levels of *Col1a2* and *Tgfb1* transcripts and TGF-β1 protein in *Rora*$^{sg/sg}$ BMT ceca at days 21 and 35 pi (Fig. 2A, B). Immunofluorescent staining for type 1 collagen (Col1) in WT BMT tissues

indicates that the most pronounced collagen deposition occurs in the submucosal (SM) region of the cecum, with more modest accumulation in the mucosa, 21 and 35 days pi. Strikingly, there is less SM Col1 staining in the *Rora*$^{sg/sg}$ BMT ceca (Fig. 2C) as quantified by evaluation of the fold change increase in surface area of SM Col1 staining normalized to total tissue surface area (Fig. 2D). Consistent with these findings, we also observe reduced type 3 collagen (Col3) staining in the submucosal regions of the cecum of *Rora*$^{sg/sg}$ BMT mice compared with WT BMT tissue (Fig. 2E). Finally, we visualized fibroblast accumulation at day 21 pi by staining for the common fibroblast markers vimentin and desmin (25). We find substantial accumulation of vimentin and desmin positive cells across the mucosal and SM regions of WT BMT ceca; desmin staining is particularly enriched within the basal lamina which is thicker in WT than in *Rora*$^{sg/sg}$ BMT samples (Fig. 2F). Quantification of vimentin^{+} and desmin^{+} cells in these immunofluorescent images reveals a reduction in fibroblast numbers in *Rora*$^{sg/sg}$ BMT cecum compared with WT BMT tissues (Fig. 2G). Taken together our results indicate that, by all criteria, *Rora*$^{sg/sg}$ BMT animals are protected from fibrosis with reduced collagen and fibroblast accumulation in the cecum.

Eosinophils and STAT6 signaling are dispensable in *Salmonella* induced fibrosis

Chronic *Salmonella* infection is known to induce a Th1/Th17 response (25), but the contribution of type 2 immune cell cytokines in this model has not been thoroughly addressed. In our cytokine analysis, however, we find that IL-5 and IL-13 transcript levels in fibrotic WT BMT cecal tissues were similar to infected tissues of *Rora*$^{sg/sg}$ BMT animals, and importantly, were reduced or unaltered when compared with uninfected samples (Fig. S1A). While we find that absolute numbers of ILC2s and indeed eosinophils in WT BMT cecal samples expand in response to *Salmonella* infection, and are significantly reduced in *Rora*$^{sg/sg}$ BMT samples, it is noteworthy that the relative proportions of ILC2s and eosinophils (as Th2 effector cells) normalized to all CD45^{+} cells are reduced or unchanged during peak fibrosis when compared to naïve controls (Fig S1B,C). Thus, these data argue against a major role of ILC2s in this fibrotic response.

To further rule out a role of Th2 immunity in *Salmonella* induced fibrosis, infections were performed in eosinophil-deficient ΔdblGATA mice. These studies reveal similar pathogen burdens in the cecum and spleen (Fig. 3A) as well as comparable evidence of pathology in MT-stained cecal sections of infected animals (Fig. 3B, C). Transcript quantification also reveals similar levels of *Col1a2*, *Tnfa*, and *Il6* in the eosinophil-deficient tissues, although *Tgfb1* and *Epx* transcripts are significantly reduced (Fig. 3D). We conclude that eosinophils are dispensable in this model.

In many examples of fibrosis, STAT6 plays an essential role as a transcriptional mediator of downstream IL-4/IL-13 receptor signaling involved in the propagation of other type 2 immune cells (1). Following infection with *Salmonella*, we find that *Stat6*$^{-/-}$ and WT animals exhibit similar pathogen burdens in the cecum and the spleen (Fig. 3E) and display a similar degree of pathology in the cecum (Fig. 3F,G). Furthermore, we observe comparable levels of *Col1a2*, *Tgfb1*, *Tnfa*, and *Il6* expression in both WT and *Stat6*$^{-/-}$cecal tissues (Fig. 3H). In aggregate, our data indicate that eosinophils and STAT6/Th2 effector function signaling are dispensable for *Salmonella*-induced gut fibrosis.

RORα mediates IL-17A and IL-22 production in chronic gut inflammation and fibrosis

Although *Rora*$^{sg/sg}$ BMT mice are known to have a profound defect in ILC2 development(22, 26), one previous study indicated that RORα is also required by Th17 cells for normal cytokine production (21). In addition, although *Rora*$^{sg/sg}$ BMT animals have normal ILC3 numbers in the small intestine and mesenteric lymph nodes (mLNs) at steady state (22), several studies have detected high *Rora* transcript levels in gut ILC3s (27, 28) or ILC3-like subsets (29, 30). Despite these observations, the importance of RORα expression in regulating ILC3s in the context of inflammatory diseases is unknown. We therefore evaluated Th17 and ILC3 associated cytokines in infected *Rora*$^{sg/sg}$ BMT ceca. These mice exhibit a decrease in cecal *Il17a* and *Il22* transcripts at days 21 and 35, and a corresponding reduction in IL-17A and IL-22 protein in cecal homogenates (Fig. 4A, B). Consistent with this observation, we previously reported significantly reduced levels of IL-17A in the lungs of *Rora*$^{sg/sg}$ BMT mice in both Ova-and HDM-induced models of allergic disease (23). We conclude that Th17-biased immune responses are highly attenuated in RORα-deficient mice.

Next, we characterized IL-17A- and IL-22-producing mLN populations by flow cytometry (Fig. S2). Total mLN ILC3 numbers are comparable in WT and *Rora*$^{sg/sg}$ BMT mLNs at 21 days pi (Fig 4C). Intriguingly, despite their normal frequency, we find highly attenuated IL-17A and IL-22 production in ILC3s of *Rora*$^{sg/sg}$ BMT mice (Fig. 4D). This is further supported by evaluation of residual, radio-resistant WT ILC3 present in the mLN of *Rora*$^{sg/sg}$ BMT chimeric mice. These cells represent roughly 10% of the mLN ILC3 as determined by allotype marker staining and produce normal levels of IL-17A and IL-22 (Fig. 4D). This suggests that defective cytokine production by *Rora*$^{sg/sg}$ ILC3s is cell-intrinsic and independent of potential alterations in the composition of the inflammatory environment. Consistent with previous characterization of RORα in Th17 cells (21), *Rora*$^{sg/sg}$ CD3$^+$ T cells isolated from mLNs of infected animals have reduced IL-17A but unaltered IL-22 production compared to WT T cells (Fig. 4E).

Peripheral blood analyses of BM chimeras reveals approximately 90% donor-derived CD45.2$^+$ cells, and 10% CD45.1$^+$ radio-resistant host-derived cells (Fig. 4F). More selective analyses of IL-17A$^+$ mLN cells in WT BMT mice reveals 73% IL-17A$^+$ cell chimerism suggesting there is a subset of tissue-specific, radio-resistant IL-17A-producing cells (Fig. 4F). Interestingly, these cells are more frequent in *Rora*$^{sg/sg}$ BMT chimeras, with only ~55% of total IL-17A$^+$ cells originating from donor BM cells. Host and donor contributions to IL-22$^+$ cells in both WT and *Rora*$^{sg/sg}$ BMT mice overlap with their respective peripheral blood chimerism indicating a lack of IL-22$^+$ cell enrichment in the tissue-resident, radio-resistant population (Fig. 4F). Consistent with mLN cell analyses, ILC3s isolated from the ceca of *Rora*$^{sg/sg}$ BMT mice have reduced IL-17A and IL-22 production compared with WT BMT ILC3s (Fig. 4G); RORα-deficient cecal CD3$^+$ T-cells also display attenuated IL-17A but normal IL-22 expression (Fig. 4H). In summary, we conclude that there is a clear defect in cytokine production by Th17 and ILC3 cells in *Rora*$^{sg/sg}$ BMT mice.

Salmonella-induced gut fibrosis is dependent on *Rora*$^+$ ILC3

To further evaluate the ILC- versus Th cell-dependent contributions to fibrosis in our experimental model, we generated mixed BM chimeras by reconstituting lethally irradiated

mice with equal numbers of BM cells from *Rag1*$^{-/-}$ mice combined with either WT or *Rora*$^{sg/sg}$ BM cells. The rationale was that co-transplanting *Rag1*$^{-/-}$ and *Rora*$^{sg/sg}$ BM cells would restore normal ILC3s (*Rag1*$^{-/-}$-derived) without altering the *Rora*$^{sg/sg}$–derived T cell compartment. At 21 days pi we find cecal and splenic *Salmonella* burdens in these mice are similar (Fig. 5A). MT-stained cecal tissues from these *Rag1*$^{-/-}$/*Rora*$^{sg/sg}$ BMT animals reveal immunopathology and fibrosis comparable to *Rag1*$^{-/-}$/WT BMT animals (Fig. 5B), including a similar degree epithelial cell hyperplasia, inflammatory infiltrates, and collagen deposition in the submucosal regions, which is represented in the pathology scores (Fig. 5C). Further, we find similar transcript levels of *Col1a2, Tgfb1, Tnfa and Il6* in infected ceca of *Rag1*$^{-/-}$/WT and *Rag1*$^{-/-}$/*Rora*$^{sg/sg}$ BMT animals (Fig. 5D). Quantification of IL-17A and IL-22 in cecal homogenates indicates that these cytokines are restored to comparable levels in *Rag1*$^{-/-}$/WT BMT and of *Rag1*$^{-/-}$/*Rora*$^{sg/sg}$ BMT samples (Fig. 5E). In summary, these data argue that *Rora*-expressing ILC3s are sufficient to cause fibrosis.

Finally, to determine if IL-17A is a critical pro-fibrotic factor in this model, we treated *Salmonella*-infected mice with neutralizing antibodies against IL-17A. Although we find that the *Salmonella* burdens in the spleens and the ceca of isotype control and anti-IL-17A treated mice were unaltered (Fig. 6A), we observe reduced pathology in the ceca of animals treated with antibodies against Il-17A (Fig. 6B) as MT-stained cecal sections exhibit an attenuation in epithelial remodeling and fibrotic scarring (Fig. 6C). Moreover, IL-17A neutralization resulted in a decrease in SM collagen accumulation (Fig. 6D). Our results indicate fibrosis during the late phases of chronic *Salmonella* infection is IL-17A dependent.

Discussion

This report provides important insights into *Rora*-dependent immune function and Crohn's-like fibrotic disease (Fig 4S). Using a model of *Salmonella* induced intestinal fibrosis, we find that hematopoietic deletion of *Rora* protects animals from fibrogenesis in the gut. Assessment of tissue pathology and cytokine analysis during the pre-fibrotic phase at day 7 pi suggests early inflammatory responses were comparable in WT and *Rora*$^{sg/sg}$ BMT animals. Furthermore, *Salmonella* burdens in the gut and spleen during initial colonization were unaltered by hematopoietic *Rora* expression. These observations suggest that RORα does not influence initial inflammatory responses, or the host's ability to clear the infection, but rather plays a specific role in generating a pro-fibrotic response in the gut during late stages of chronic *Salmonella* infection. The apparent disconnect between bacterial colonization the severity of fibrosis is consistent with previous reports which demonstrate that intestinal fibrosis does not require the presence of *Salmonella* as a persistent inflammatory stimulus (31, 32). Instead, the pathology becomes self-propagating and is largely irrespective of interventions that attempt to reduce pathogen burdens or repress early inflammatory responses.

Although gut fibrosis that develops following chronic *Salmonella* infection strongly correlates with a Th17 response (25), we initially sought to examine the contributions of type 2 immune cell-associated cytokines in fibrosis. This is relevant for several reasons. First, in a mouse model of TNBS-induced colitis, peak IL-4 and IL-13 cytokine levels were reported during the late phases of inflammation and were associated with tissue remodeling

and fibrosis (4). Second, ILC2s are well known to recruit eosinophils by their secretion of IL-5 (33); eosinophilia has been linked previously to stricture complications in CD patients and IL-13 has been reported to promote gut fibroblast activation (16). Therefore, while it is likely ILC2s are irrelevant during the early phase of *Salmonella* infection, their role in downstream fibrotic remodeling has not been thoroughly investigated. While we observed a profound attenuation in collagen deposition in infected $Rora^{sg/sg}$ BMT ILC2 deficient animals, IL-13 and IL-5 levels were not markedly altered in fibrotic gut tissue when compared to uninfected controls. In support of these observations, we find that fibrosis is not diminished in cecal tissues of infected ΔdblGATA or $Stat6^{-/-}$ mice, which suggests that eosinophils and STAT6 signaling as mediators of Th2 effector cell functions are dispensable for *Salmonella*-induced fibrosis. Theses findings argue strongly for a Th2/ILC2-independent role for RORα in fibrosis. In examining other eosinophil derived factors previously implicated in IBD, the reduction in *Epx1* was fully expected since infected ΔdblGATA mice lack eosinophils and therefore, this selective marker. Eosinophils are also a well-known source of TGF-β1 and therefore it is perhaps not surprising that its production is lower in these animals. The fact that loss of eosinophils as a source of TGF-β1 has no effect on the fibrotic outcome, however, is intriguing. One could argue that the residual levels of TGF-β1 we observe in the eosinophil-deficient mice is necessary but not sufficient to induce fibrosis and that a second signal is required. Based on our antibody suppression experiments we would argue that IL-17A is one such factor and a critical driver of fibrotic disease.

Consistent with a previous report identifying RORα as an important transcriptional mediator of Th17 cell cytokine production (21), we find that IL-17A and IL-22 levels were diminished in infected cecal tissue of $Rora^{sg/sg}$ BMT mice compared with WT samples. Interestingly, normal IL-17A and IL-22 production by ILC3s is *Rora* dependent while IL-17A expression by T cells is also impaired in *Salmonella*-infected $Rora^{sg/sg}$ BMT animals. This defect in cytokine production by RORα-deficient ILC3s and Th17 cells is further illustrated by a ~50% increase in the relative proportion of radio-resistant, host-derived IL-17$^+$ cell numbers in mLNs of $Rora^{sg/sg}$ BMT animals when compared to WT controls. The persistence of WT radio-resistant subsets represents a caveat in our BMT model. However, despite the presence of a larger relative population of IL-17A producing radio-resistant host-derived cells, the cumulative effect of deleting *Rora* in donor cells is sufficient to attenuate the fibrotic phenotype. To delineate the contributions of ILC3s and Th17 cells to the phenotype in our disease model, we restored WT innate cells by co-transplanting mixed $Rag1^{-/-}$ and $Rora^{sg/sg}$ BM cells into recipient animals. Following *Salmonella* infection, these mice develop fibrotic disease in the gut and have IL-17A and IL-22 levels similar to their $Rag1^{-/-}$/WT BMT counterparts. These data demonstrates that ILC3s are sufficient to cause fibrosis, but does not formally rule out an additional role of Th17 cells. New technological approaches to selectively deplete ILC3s or ablate *Rora* in ILC3s would be necessary to definitively address this question.

While we have shown that antibody mediated neutralization of IL-17A protects against fibrosis in a *Salmonella*-induced model, the clinical importance of these findings may be questioned since anti-IL-17A antibody treatment failed as a therapy in a clinical trial of Crohn's disease patients due to lack of efficacy and adverse side effects (34). However, Crohn's disease manifests itself in many ways and fibrosis is only detected in a subset of

these patients. Importantly, patients with "stricture causing obstructive symptoms" were excluded from this clinical trial. With this in mind, we would argue that the effects of anti-IL-17A on stricture formation and maintenance in humans remain an open question and that further study is justified.

Although RORα and RORγt are related members of a subfamily of nuclear orphan receptors, each possess distinct and some overlapping functions in hematopoietic development. Unlike *Rorc* deletion, which ablates ILC3s and Th17 cells, the effect of *Rora* deletion on these subsets appears to be far more subtle and limited to an attenuation of cytokine production. There has been strong interest in developing RORγt inhibitors as a therapy for Th17- or ILC3- mediated disorders (35–37). However, there are some concerns with this strategy as RORγt^{+} regulatory T cells were found to be critical in limiting disease severity in experimental colitis (38, 39). Moreover, RORγt regulates thymocyte differentiation and aged *Rorc*$^{-/-}$ mice exhibit a very high frequency of T cell lymphoma (40). Our findings argue that RORα may serve as a more attractive therapeutic target for Crohn's disease associated fibrosis and that development of selective inhibitors of RORα (that spare RORγt) is warranted.

Materials and Methods

Study design

Our aim was to investigate the role of RORα dependent immunity in gut fibrotic responses. We employed a bone marrow transplant model for hematopoietic *Rora* deficiency in mice as well as other conventional mutant knockout strains in a chronic infection model of intestinal fibrosis. Age and sex matched mice were randomly divided into recipient groups for BM transplantation. Infection experiments included four to eight mice per group and were performed at least two times with the exception of experiments pertaining to *Stat6*$^{-/-}$ mice (Fig. 3E–3H), which were from a single experiment.

Mice

C57BL/6J, B6.SJL-Ptprc^{a}Pepc^{b}/BoyJ (CD45.1), B6.C3(Cg)-*Rora*^{sg}/J (*Rora*$^{sg/sg}$), C.129S1(B6)-*Gata1*^{tm6Sho}/J (ΔdblGATA), C.129S2-*Stat6*^{tm1Gru}/J (*Stat6*$^{-/-}$), and B6.129S7-*Rag1*^{tm1Mom}/J (*Rag1*$^{-/-}$) mice were maintained in a specific pathogen-free environment at the Biomedical Research Centre. BM chimeras were generated by lethally irradiating and reconstituting CD45.1 animals with two million BM cells isolated from WT or *Rora*$^{sg/sg}$ littermates. For *Rag1*$^{-/-}$ co-transplant experiments, WT or *Rora*$^{sg/sg}$ BM cells were mixed 1:1 with *Rag1*$^{-/-}$ BM cells for reconstitution. Animals were used at least 8 weeks after transplantation. All experiments performed were approved by the UBC Animal Care Committee.

Infection model

Mice were treated with 20 mg of streptomycin by oral gavage 24 hours prior to oral infection with 3×10^{6} *Salmonella* Typhimurium Δ*aroA* CFU in 100 μL PBS. At various time points, tissues were collected and homogenized in sterile PBS; serial dilutions of the homogenates were plated on LB agar plates (100 μg/mL streptomycin) for bacterial

enumeration. For IL-17A neutralizing experiments, mice were injected intraperitoneally with 200 μg of antibodies against IL-17A (Janssen, CNTO 8096), or isotype control (Janssen, CNTO 2407) three times per week beginning at 7 days after infection, and sacrificed at day 21 pi for tissue collection.

Histology and immunohistochemistry

Formalin fixed and paraffin embedded tissues were cut into 5-μm sections for Masson's trichrome (MT) staining. Cecal pathology was scored as previously described (25). For immunostaining, tissue sections were deparaffinized, rehydrated, and underwent antigen retrieval; antibodies against type 1 collagen (ABcam), type 3 collagen (Fitzgerald), vimentin (ABcam), and desmin (Santa Cruz) were used, followed by incubation with Alexa Fluor-conjugated secondaries (Life Technologies). Sections were then mounted using ProLong Gold Antifade with DAPI (Life Technologies). Optical z-stack images were captured on a Leica SP5X confocal microscope and analyzed using ImageJ.

Quantitative RT-PCR

Total RNA extracted from terminal ends of cecal tissue using Trizol (Invitrogen) was reverse transcribed with a high-capacity cDNA RT kit (Thermo). Quantitative real-time PCR was performed using SYBR green chemistry (KAPA) and gene-specific primer pairs (supplemental table 1) on an AB7900 RT-PCR system.

Cytokine detection

Concentrations of TNF, IL-6, MCP-1, IFN-γ, IL-12p70, IL-10, and IL-17A in cecal homogenates were determined using a cytometric bead array (BD Biosciences); TGF-β1 and IL-22 levels were determined by plate ELISA kits (eBiosciences) according to manufacturer's instructions.

Immune analysis and flow cytometry

Mesenteric lymph nodes were excised and passed through a 70-μm filter to generate single cell suspensions. Leukocytes were isolated from ceca by flushing luminal contents, mincing and incubating tissues in 1.5 U/mL collagenase D and 2.4 U/mL dispase II (Roche) for 30 minutes at 37°C with gentle rotation; samples were then passed through a 70 μm filter and hematopoietic cells were enriched by Percoll (GE) separation. Cells were restimulated using 50 ng/mL PMA and 750 ng/mL ionomycin (Sigma) in the presence of brefeldin A (eBiosciences) for 4 hours. Samples were then incubated with 5 μg/mL anti-CD16/32 (2.4G2, in house) to block non-specific antibody binding. Fluorescence-conjugated antibodies to CD45.2 (104), CD8 (53.67), CD11b (M1/70), CD11c (N418), CD19 (1D3), NK1.1 (PK136), Gr1 (RB6-8C5), Ter119, CD3e (145-2C11), CD90.2 (30-H12), KLRG1 (2F1), Sca-1 (D7), IL-17A (eBio17B7), and IL-22 (1H8PWSR) were used. A fixation and permeabilization buffer set (eBiosciences) was used for intracellular cytokine staining and a fixable viability dye (eBiosciences) was used for dead cell exclusion. Data was acquired on a BD LSRII, and analyzed using FlowJo.

Statistics

Results are presented as mean +/− SEM; statistical significance was determined by unpaired Student's *t* test.

Supplementary Material

Refer to Web version on PubMed Central for supplementary material.

Acknowledgments

We thank BRC core members Ingrid Barta (histology), Taka Murakami (genotyping), Wei Yuan (animal care), Mike Williams (protein), A. Johnson, J. Wong (flow cytometry), Rupi Dhesi, and Les Rollins (media); Dr. Bruce Vallance for providing the *S.* Typhymurium Δ*aroA* strain and guidance in the Crohn's model; and Dr. Georgia Perona-Wright for the *Stat6*$^{-/-}$ mice.

Funding: This work was funded by the AllerGen NCE (Strategic Initiative grant, KMM), CIHR (KMM, MOP-137142). Funding for B.C.L. provided by a UBC 4YF; M.J.G. was supported by an AllerGen CAIDATI award.

References

1. Wynn TA. Cellular and molecular mechanisms of fibrosis. J Pathol. 2008; 214:199–210. [PubMed: 18161745]
2. Rieder F, Fiocchi C. Intestinal fibrosis in IBD—a dynamic, multifactorial process. Nat Rev Gastroenterol Hepatol. 2009; 6:228–235. [PubMed: 19347014]
3. Fallon PG, Richardson EJ, McKenzie GJ, McKenzie AN. Schistosome infection of transgenic mice defines distinct and contrasting pathogenic roles for IL-4 and IL-13: IL-13 is a profibrotic agent. J Immunol. 2000; 164:2585–2591. [PubMed: 10679097]
4. Fichtner-Feigl S, Fuss IJ, Young CA, Watanabe T, Geissler EK, Schlitt HJJ, Kitani A, Strober W. Induction of IL-13 triggers TGF-beta1-dependent tissue fibrosis in chronic 2,4,6-trinitrobenzene sulfonic acid colitis. J Immunol. 2007; 178:5859–5870. [PubMed: 17442970]
5. Sonnenberg GF, Artis D. Innate lymphoid cells in the initiation, regulation and resolution of inflammation. Nat Med. 2015; 21:698–708. [PubMed: 26121198]
6. Hams E, Armstrong ME, Barlow JL, Saunders SP, Schwartz C, Cooke G, Fahy RJ, Crotty TB, Hirani N, Flynn RJ, Voehringer D, McKenzie ANJ, Donnelly SC, Fallon PG. IL-25 and type 2 innate lymphoid cells induce pulmonary fibrosis. Proc Natl Acad Sci USA. 2014; 111:367–372. [PubMed: 24344271]
7. Monticelli LA, Sonnenberg GF, Abt MC, Alenghat T, Ziegler CGK, Doering TA, Angelosanto JM, Laidlaw BJ, Yang CY, Sathaliyawala T, Kubota M, Turner D, Diamond JM, Goldrath AW, Farber DL, Collman RG, Wherry JE, Artis D. Innate lymphoid cells promote lung-tissue homeostasis after infection with influenza virus. Nat Immunol. 2011; 12:1045–1054. [PubMed: 21946417]
8. Monticelli LA, Osborne LC, Noti M, Tran SV, Zaiss DMW, Artis D. IL-33 promotes an innate immune pathway of intestinal tissue protection dependent on amphiregulin–EGFR interactions. Proc Natl Acad Sci USA. 2015; 112:10762–10767. [PubMed: 26243875]
9. Satoh-Takayama N, Vosshenrich C, Lesjean-Pottier S, Sawa S, Lochner M, Rattis F, Mention JJ, Thiam K, Cerf-Bensussan N, Mandelboim O, Eberl G, Santo JP. Microbial Flora Drives Interleukin 22 Production in Intestinal NKp46+ Cells that Provide Innate Mucosal Immune Defense. Immunity. 2008; 29:958–970. [PubMed: 19084435]
10. Gladiator A, Wangler N, Trautwein-Weidner K, LeibundGut-Landmann S. Cutting edge: IL-17-secreting innate lymphoid cells are essential for host defense against fungal infection. J Immunol. 2013; 190:521–525. [PubMed: 23255360]
11. Aparicio-Domingo P, Romera-Hernandez M, Karrich JJ, Cornelissen F, Papazian N, Lindenbergh-Kortleve DJ, Butler JA, Boon L, Coles MC, Samsom JN, Cupedo T. Type 3 innate lymphoid cells

maintain intestinal epithelial stem cells after tissue damage. J Exp Med. 2015; 212:1783–1791. [PubMed: 26392223]

12. Kirchberger S, Royston DJ, Boulard O, Thornton E, Franchini F, Szabady RL, Harrison O, Powrie F. Innate lymphoid cells sustain colon cancer through production of interleukin-22 in a mouse model. J Exp Med. 2013; 210:917–931. [PubMed: 23589566]
13. Baumgart DC, Sandborn WJ. Crohn's disease. The Lancet. 2012; 380:1590–1605.
14. Geremia A, Arancibia-Cárcamo CV, Fleming M, Rust N, Singh B, Mortensen NJ, Travis S, Powrie F. IL-23–responsive innate lymphoid cells are increased in inflammatory bowel disease. J Exp Med. 2011; 208:1127–1133. [PubMed: 21576383]
15. Mizuno S, Mikami Y, Kamada N, Handa T, Hayashi A, Sato T, Matsuoka K, Matano M, Ohta Y, Sugita A, Koganei K, Sahara R, Takazoe M, Hisamatsu T, Kanai T. Cross-talk between RORγt+ innate lymphoid cells and intestinal macrophages induces mucosal IL-22 production in Crohn's disease. Inflamm Bowel Dis. 2014; 20:1426–1434. [PubMed: 24991784]
16. Masterson JC, Capocelli KE, Hosford L, Biette K, McNamee EN, de Zoeten EF, Harris R, Fernando SD, Jedlicka P, Protheroe C, Lee JJ, Furuta GT. Eosinophils and IL-33 Perpetuate Chronic Inflammation and Fibrosis in a Pediatric Population with Stricturing Crohn's Ileitis. Inflamm Bowel Dis. 2015; 21:2429. [PubMed: 26218140]
17. Bailey JR, Bland PW, Tarlton JF, Peters I, Moorghen M, Sylvester PA, Probert CSJ, Whiting CV. IL-13 Promotes Collagen Accumulation in Crohn's Disease Fibrosis by Down-Regulation of Fibroblast MMP Synthesis: A Role for Innate Lymphoid Cells? PLoS ONE. 2012; 7:e52332. [PubMed: 23300643]
18. Ivanov, McKenzie BS, Zhou L, Tadokoro CE, Lepelley A, Lafaille JJ, Cua DJ, Littman DR. The orphan nuclear receptor RORgammat directs the differentiation program of proinflammatory IL-17+ T helper cells. Cell. 2006; 126:1121–1133. [PubMed: 16990136]
19. Sanos SL, Bui VL, Mortha A, Oberle K, Heners C, Johner C, Diefenbach A. RORgammat and commensal microflora are required for the differentiation of mucosal interleukin 22-producing NKp46+ cells. Nat Immunol. 2009; 10:83–91. [PubMed: 19029903]
20. Sawa S, Cherrier M, Lochner M, Satoh-Takayama N, Fehling HJ, Langa F, Di Santo JP, Eberl G. Lineage relationship analysis of RORgammat+ innate lymphoid cells. Science. 2010; 330:665–669. [PubMed: 20929731]
21. Yang XO, Pappu BP, Nurieva R, Akimzhanov A, Kang HS, Chung Y, Ma L, Shah B, Panopoulos AD, Schluns KS, Watowich SS, Tian Q, Jetten AM, Dong C. T helper 17 lineage differentiation is programmed by orphan nuclear receptors ROR alpha and ROR gamma. Immunity. 2008; 28:29–39. [PubMed: 18164222]
22. Halim T, MacLaren A, Romanish MT, Gold MJ, McNagny KM, Takei F. Retinoic-Acid-Receptor-Related Orphan Nuclear Receptor Alpha Is Required for Natural Helper Cell Development and Allergic Inflammation. Immunity. 2012; 37:463–474. [PubMed: 22981535]
23. Gold MJ, Antignano F, Halim T, Hirota JA, Blanchet M-R, Zaph C, Takei F, McNagny KM. Group 2 innate lymphoid cells facilitate sensitization to local, but not systemic, TH2-inducing allergen exposures. J Allergy Clin Immunol. 2014; 133:1142–1148. [PubMed: 24679471]
24. Halim TY, Steer CA, Matha L, Gold MJ, Martinez-Gonzalez I, McNagny KM, McKenzie AN, Takei F. Group 2 innate lymphoid cells are critical for the initiation of adaptive T helper 2 cell-mediated allergic lung inflammation. Immunity. 2014; 40:425–435. [PubMed: 24613091]
25. Grassl GA, Valdez Y, Bergstrom K, Vallance BA, Finlay BB. Chronic Enteric Salmonella Infection in Mice Leads to Severe and Persistent Intestinal Fibrosis. Gastroenterol. 2008; 134:768–780.
26. Wong SH, Walker JA, Jolin HE, Drynan LF, Hams E, Camelo A, Barlow JL, Neill DR, Panova V, Koch U, Radtke F, Hardman CS, Hwang YY, Fallon PG, McKenzie AN. Transcription factor RORalpha is critical for nuocyte development. Nat Immunol. 2012; 13:229–236. [PubMed: 22267218]
27. Hoyler T, Klose C, Souabni A, Turqueti-Neves A, Pfeifer D, Rawlins EL, Voehringer D, Busslinger M, Diefenbach A. The Transcription Factor GATA-3 Controls Cell Fate and Maintenance of Type 2 Innate Lymphoid Cells. Immunity. 2012; 37:634–648. [PubMed: 23063333]
28. Robinette ML, Fuchs A, Cortez VS, Lee JS, Wang Y, Durum SK, Gilfillan S, Colonna M, Shaw L, Yu B, Goldrath A, Mostafavi S, Regev A, Kim EY, Dwyer DF, Brenner MB, Austen FK, Rhoads

A, Moodley D, Yoshida H, Mathis D, Benoist C, Nabekura T, Lam V, Lanier LL, Brown B, Merad M, Cremasco V, Turley S, Monach P, Dustin ML, Li Y, Shinton SA, Hardy RR, Shay T, Qi Y, Sylvia K, Kang J, Fairfax K, Randolph GJ, Robinette ML, Fuchs A, Colonna M. Transcriptional programs define molecular characteristics of innate lymphoid cell classes and subsets. Nat Immunol. 2015; 16:306–317. [PubMed: 25621825]

29. Luci C, Reynders A, Ivanov, Cognet C, Chiche L, Chasson L, Hardwigsen J, Anguiano E, Banchereau J, Chaussabel D, Dalod M, Littman DR, Vivier E, Tomasello E. Influence of the transcription factor RORgammat on the development of NKp46+ cell populations in gut and skin. Nat Immunol. 2009; 10:75–82. [PubMed: 19029904]
30. Allan DSJ, Kirkham CL, Aguilar OA, Qu LC, Chen P, Fine JH, Serra P, Awong G, Gommerman JL, Zúñiga-Pflücker JC, Carlyle JR. An in vitro model of innate lymphoid cell function and differentiation. Mucosal Immunology. 2015; 8:340–351. [PubMed: 25138665]
31. Månsson LE, Montero M, Zarepour M, Bergstrom KS, Ma C, Huang T, Man C, Grassl GA, Vallance BA. MyD88 signaling promotes both mucosal homeostatic and fibrotic responses during Salmonella-induced colitis. Am J Physiol Gastrointest Liver Physiol. 2012; 303
32. Johnson LA, Luke A, Sauder K, Moons DS, Horowitz JC, Higgins PD. Intestinal fibrosis is reduced by early elimination of inflammation in a mouse model of IBD: impact of a "Top-Down" approach to intestinal fibrosis in mice. Inflamm Bowel Dis. 2012; 18:460–471. [PubMed: 21761511]
33. Imai Y, Yasuda K, Sakaguchi Y, Haneda T, Mizutani H, Yoshimoto T, Nakanishi K, Yamanishi K. Skin-specific expression of IL-33 activates group 2 innate lymphoid cells and elicits atopic dermatitis-like inflammation in mice. Proc Natl Acad Sci USA. 2013; 110:13921–13926. [PubMed: 23918359]
34. Hueber W, Sands BE, Lewitzky S, Vandemeulebroecke M, Reinisch W, Higgins PD, Wehkamp J, Feagan BG, Yao MD, Karczewski M, Karczewski J, Pezous N, Bek S, Bruin G, Mellgard B, Berger C, Londei M, Bertolino AP, Tougas G, Travis SP. G. Secukinumab in Crohn's Disease Study. Secukinumab, a human anti-IL-17A monoclonal antibody, for moderate to severe Crohn's disease: unexpected results of a randomised, double-blind placebo-controlled trial. Gut. 2012; 61:1693–1700. [PubMed: 22595313]
35. de Wit J, Al-Mossawi MH, Huhn MH, Arancibia-Carcamo CV, Doig K, Kendrick B, Gundle R, Taylor P, McClanahan T, Murphy E, Zhang H, Barr K, Miller JR, Hu X, Aicher TD, Morgan RW, Glick GD, Zaller D, Correll C, Powrie F, Bowness P. RORgammat inhibitors suppress TH17 responses in inflammatory arthritis and inflammatory bowel disease. J Allergy Clin Immunol. 2016; 137:960–963. [PubMed: 26611672]
36. Withers DR, Hepworth MR, Wang X, Mackley EC, Halford EE, Dutton EE, Marriott CL, Brucklacher-Waldert V, Veldhoen M, Kelsen J, Baldassano RN, Sonnenberg GF. Transient inhibition of ROR-gammat therapeutically limits intestinal inflammation by reducing TH17 cells and preserving group 3 innate lymphoid cells. Nat Med. 2016; 22:319–323. [PubMed: 26878233]
37. Solt LA, Kumar N, Nuhant P, Wang Y, Lauer JL, Liu J, Istrate MA, Kamenecka TM, Roush WR, Vidovic D, Schurer SC, Xu J, Wagoner G, Drew PD, Griffin PR, Burris TP. Suppression of TH17 differentiation and autoimmunity by a synthetic ROR ligand. Nature. 2011; 472:491–494. [PubMed: 21499262]
38. Sefik E, Geva-Zatorsky N, Oh S, Konnikova L, Zemmour D, McGuire AM, Burzyn D, Ortiz-Lopez A, Lobera M, Yang J, Ghosh S, Earl A, Snapper SB, Jupp R, Kasper D, Mathis D, Benoist C. Individual intestinal symbionts induce a distinct population of RORgamma(+) regulatory T cells. Science. 2015; 349:993–997. [PubMed: 26272906]
39. Ohnmacht C, Park JH, Cording S, Wing JB, Atarashi K, Obata Y, Gaboriau-Routhiau V, Marques R, Dulauroy S, Fedoseeva M, Busslinger M, Cerf-Bensussan N, Boneca IG, Voehringer D, Hase K, Honda K, Sakaguchi S, Eberl G. The microbiota regulates type 2 immunity through RORgammat(+) T cells. Science. 2015; 349:989–993. [PubMed: 26160380]
40. Ueda E, Kurebayashi S, Sakaue M, Backlund M, Koller B, Jetten AM. High incidence of T-cell lymphomas in mice deficient in the retinoid-related orphan receptor RORgamma. Cancer Res. 2002; 62:901–909. [PubMed: 11830550]

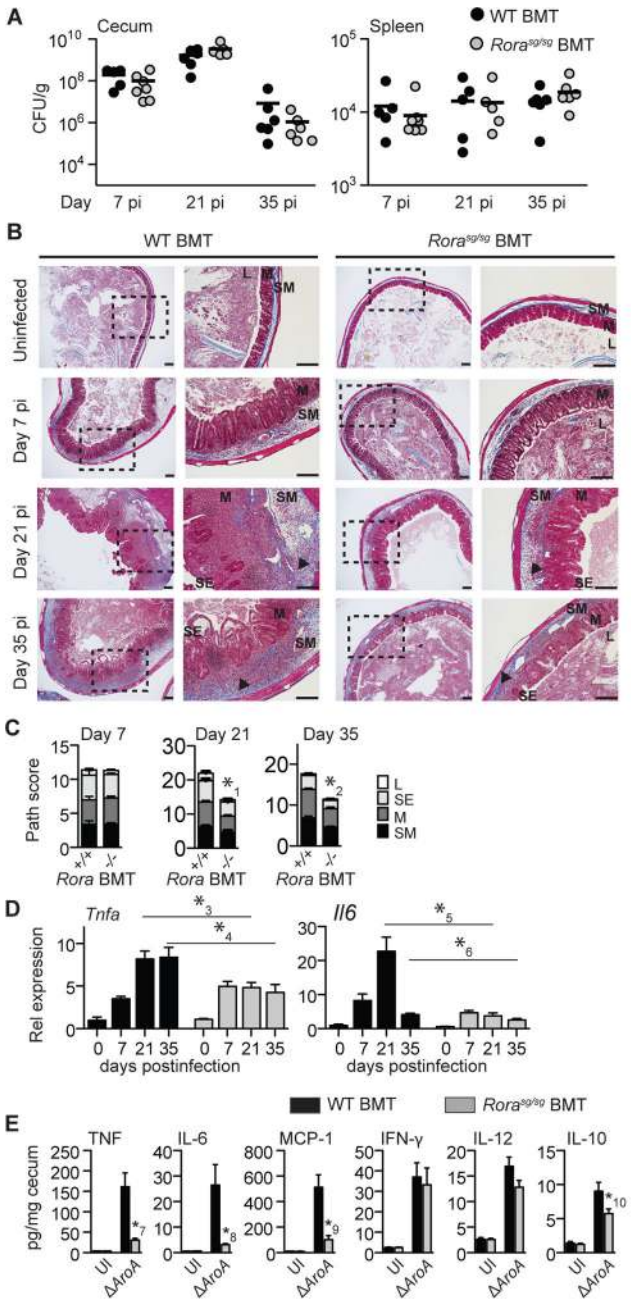

Figure 1. Hematopoietic expression of *Rora* mediates *S.* Typhimurium Δ*aroA* driven cecal immunopathology and fibrosis

WT and *Rora*$^{sg/sg}$ BMT mice were infected with *Salmonella* and sacrificed 7, 21, and 35 days pi. (A) *Salmonella* colonization of ceca and spleens of infected animals. CFU, colony-forming unit. (B) Masson's trichrome (MT)-stained cecal tissue sections. L, lumen; SE, surface epithelium; M, mucosa; SM, submucosa. Arrowheads indicate submucosal collagen accumulation visualized by blue staining. Scale bar, 200 μm. (C) Pathology scores of the luminal, epithelial, mucosal, and submucosal subsections of cecal tissue. *1, p = 0.012 (n=5 per group); *2, p= 0.0016 (n=6, 7 per group). (D) Transcript levels of pro-inflammatory

cytokines *Tnfa* and *Il6* in ceca normalized to *Gapdh*. TNFa: *3, p=0.022 (n=5 per group); *4, p=0.027 (n=5, 6 per group); *5, p=0.002 (n=5 per group); *6, p = 0.032 (n=11, 13 per group; data from 2 independent experiments) (E) Protein levels of TNF, IL-6, MCP-1, IFN-γ, IL-12p70, and IL-10 in naïve and 21 days pi cecal homogenates as determined by cytometric bead array (CBA) normalized to total tissue protein. *7, p=0.0017; *8, p=0.012; *9, p=0.0010; *10, p=0.040 (n=10, 11; data from 2 independent experiments). Significance determined by unpaired student's t test.

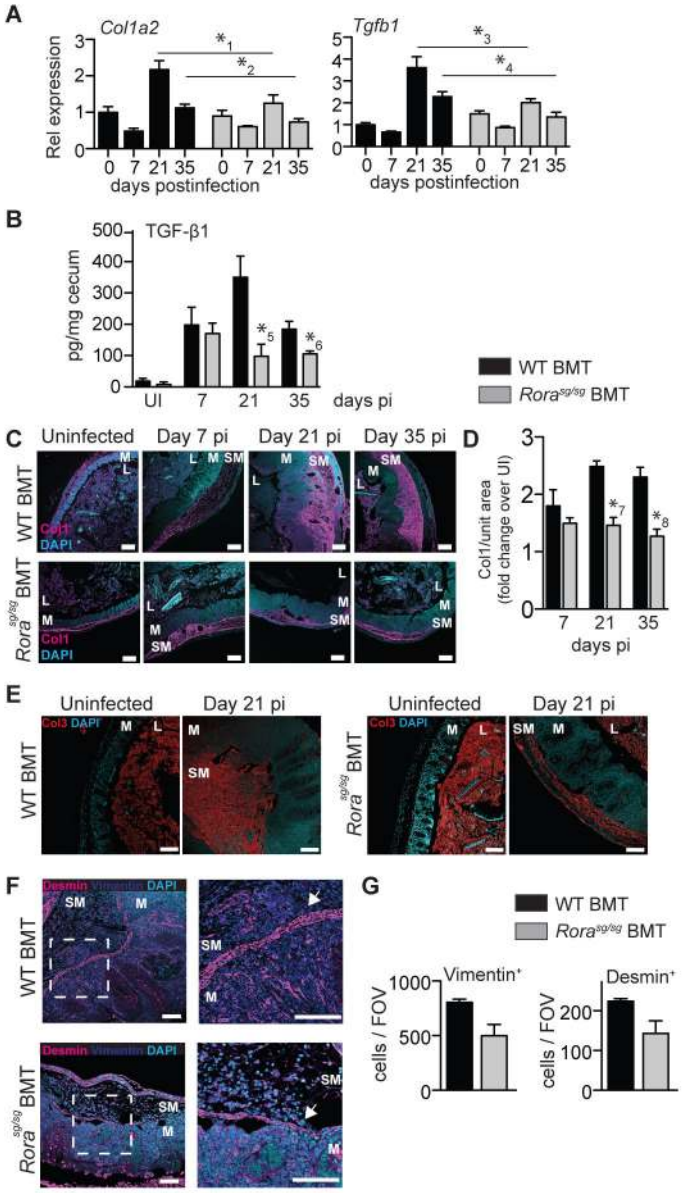

Figure 2. Attenuated collagen deposition and reduced fibroblast cell numbers in cecal tissue of chronically infected *Rora*$^{sg/sg}$ BMT animals

(A) Cecal transcript levels of *Col1a2* and *Tgfb1* normalized to *Gapdh*. *1, p=0.026 (n=5 per group); *2, p=0.016 (n=6,7 per group); *3, p=0.029 (n=5 per group); *4, p=0.015 (n=6, 7 per group) (B) TGF-β1 protein levels of cecal homogenates normalized to total protein. *5, p=0.0044 (n=10 per group, data from 2 independent experiments); *6, p=0.023 (n=5, 6 per group) (C) Immunofluorescence images of cecal sections stained for type 1 collagen (Col1, magenta) and nuclei (DAPI, cyan). Scale bar, 100 μm. (D) Quantification of the submucosal collagen surface area normalized to total tissue surface area expressed as fold change of uninfected. *7, p=2.96×10^{-4} (n=5 per group); *8, p= 5.57×10^{-4} (n=6, 7 per group) (E) Immunofluorescence images of cecal sections stained for type 3 collagen (Col3, red) and nuclei (DAPI, cyan). Scale bar, 100 μm. (F) Desmin (magenta), vimentin (blue), and nuclear

(DAPI, cyan) staining for fibroblasts in cecal tissues 21 days pi. Arrowheads indicate desmin$^+$ staining in the basal lamina. Scale bar, 100 μm. (G) Quantification of vimentin$^+$ or desmin$^+$ fibroblasts per representative field of view (FOV). Significance determined by unpaired Student's *t* test.

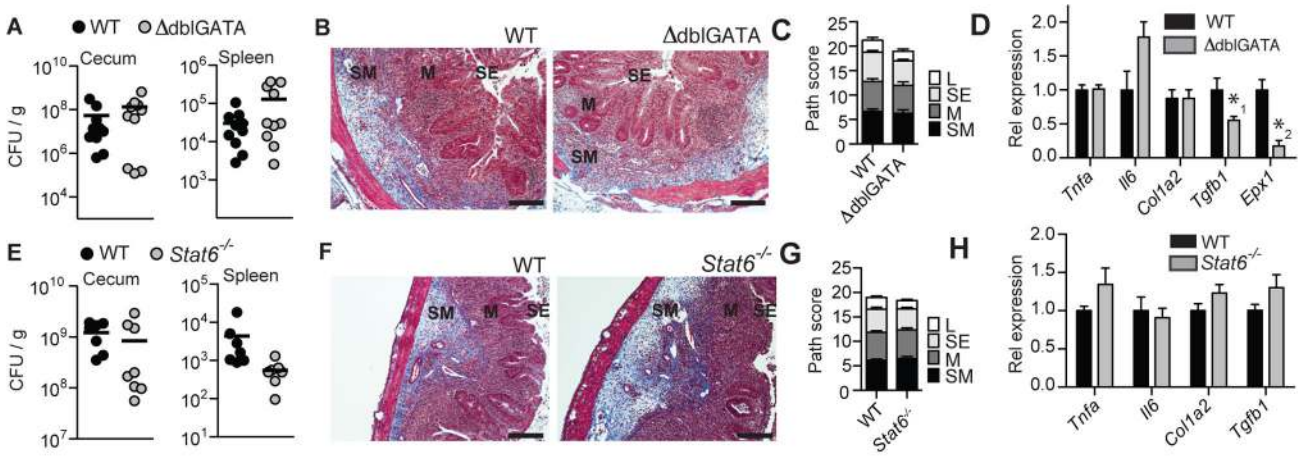

Figure 3. Eosinophils and STAT6 signaling are dispensable in *S.* Typhimurium Δ*aroA*-dependent gut inflammation and fibrosis

(A–D) Eosinophil deficient ΔdblGATA, (E–H) *Stat6*$^{-/-}$ and their respective WT controls were infected with *Salmonella* and sacrificed 21 days pi. (A) Cecal and splenic *Salmonella* burdens of infected animals. (n=10 per group; data from two independent experiments) (B) MT-stained cecal sections and (C) their corresponding pathology scores. (D) Transcript levels of *Tnfa, Il6, Col1a2, Tgfb1,* and *Epx* of infected cecal tissues normalized to *Gapdh*. *1, p=0.042; *2, p=0.0014 (n=5 per group). Significance determined by unpaired student's t test. (E) Pathogen burdens of *Salmonella* infected ceca and spleens. (n=7, 8; data from single experiment. (F) MT-stained infected cecal tissues and (G) their corresponding pathological scores. (H) Transcript levels of *Tnfa, Il6*, *Col1a2*, and *Tgfb1* of *Salmonella* infected ceca normalized to *Gapdh*. Scale bar, 200 μm.

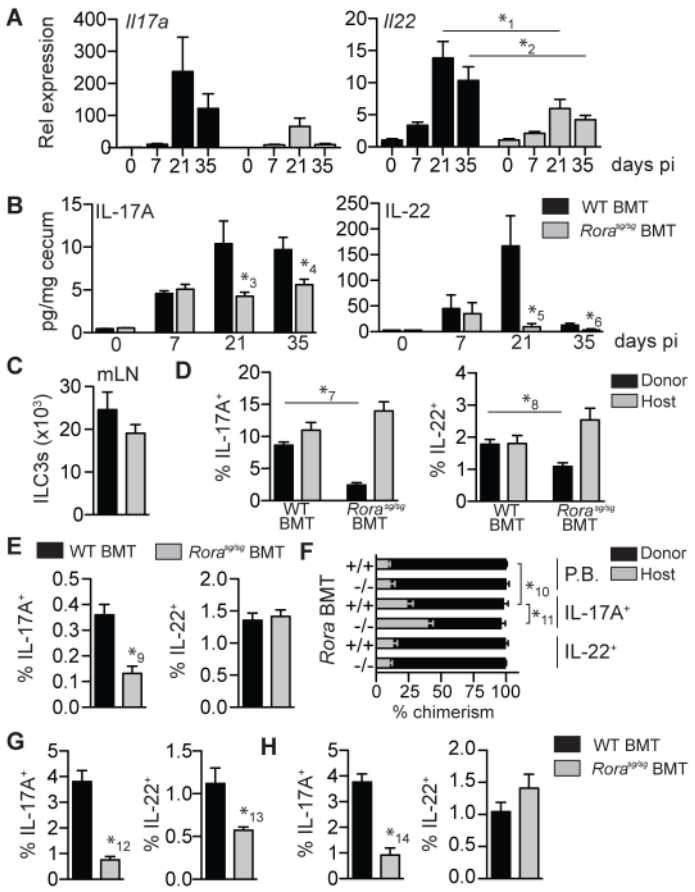

Figure 4. ILC3 production of IL-17A and IL-22 is *Rora* dependent in response to chronic *Salmonella* infection

(A) Transcripts of *Il17a* and *Il22* in WT and *Rora*$^{sg/sg}$ BMT ceca normalized to *Gapdh*. *1, p=0.029 (n=5 per group); *2, p=0.018 (n= 11, 13 per group; data from two independent experiments) (B) Protein levels of IL-17A and IL-22 in cecal homogenates normalized to total protein. *3, p=0.035 (n=10 per group; data from two independent experiments); *4, p=0.034 (n=6, 7 per group); *5, p = 0.020 (n=10, 11 per group; data from two independent experiment); *6, p=0.036 (n=6 per group). (C) Total ILC3s (CD45^{+} Lin^{neg} CD90^{high} KLRG1^{neg}) per mLN 21 days pi. (D–F) Intracellular staining of IL-17A and IL-22 of mLN leukocyte subsets following restimulation with PMA, ionomycin, and BFA. Donor versus recipient hematopoietic cells determined by expression of congenic CD45. Percentages of IL-17A^{+} and IL-22^{+} mLN ILC3s (D) and CD3e^{+} lymphocytes (E). (F) Comparison of peripheral blood chimerism with percent contribution of total IL-17A^{+} or IL22^{+} events from BM-donor derived versus radio-resistant recipient hematopoietic cells. *7, p=1.14×10^{-6}; *8, p= 0.0041; *9, p=6.98×10^{-4}; *10, p=0.0022; *11, p=0.0056 (n=5, 7 per group). One of three independent experiments. Percentages of IL-17A^{+} and IL-22^{+} gut ILC3s (G) and CD3e^{+} lymphocytes (H). *12, p=1.29×10^{-4}; *13, p= 0.035; *14, p=1.17×10^{-4} (n=5 per group). One of two independent experiments. Significance determined by unpaired Student's *t* test.

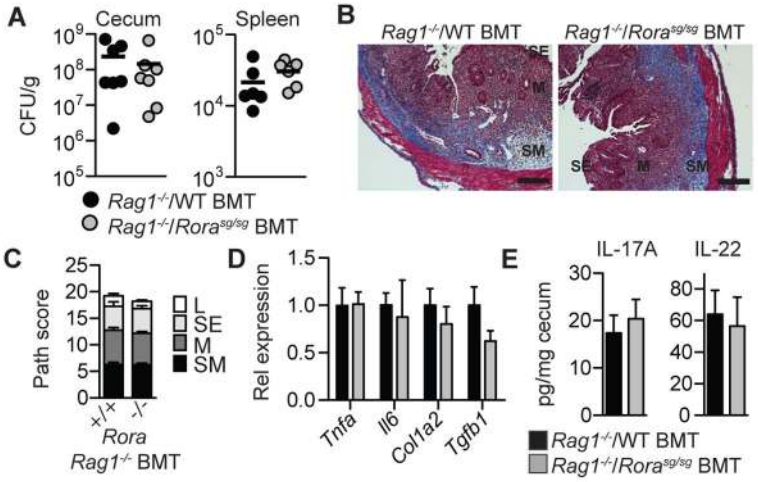

Figure 5. Restoring the innate cell compartment in *Rora*$^{sg/sg}$ BMT mice is sufficient to cause fibrosis

S. Typhimurium Δ*aroA* infection of *Rag1*$^{-/-}$/WT and *Rag1*$^{-/-}$/*Rora*$^{sg/sg}$ mixed BMT chimeras. (A) Bacterial counts of ceca and spleens 21 days pi. (B) MT-stained cecal tissue with (C) corresponding pathology scores. (D) Relative mRNA expression of *Tnfa, Il6, Col1a2*, and *Tgfb1* in infected ceca normalized to *Gapdh*. (E) IL-17A and IL-22 protein quantification in cecal homogenates. Representative data from two independent experiments (n = 5 or 7 per experiment). Scale bar, 200 μm.

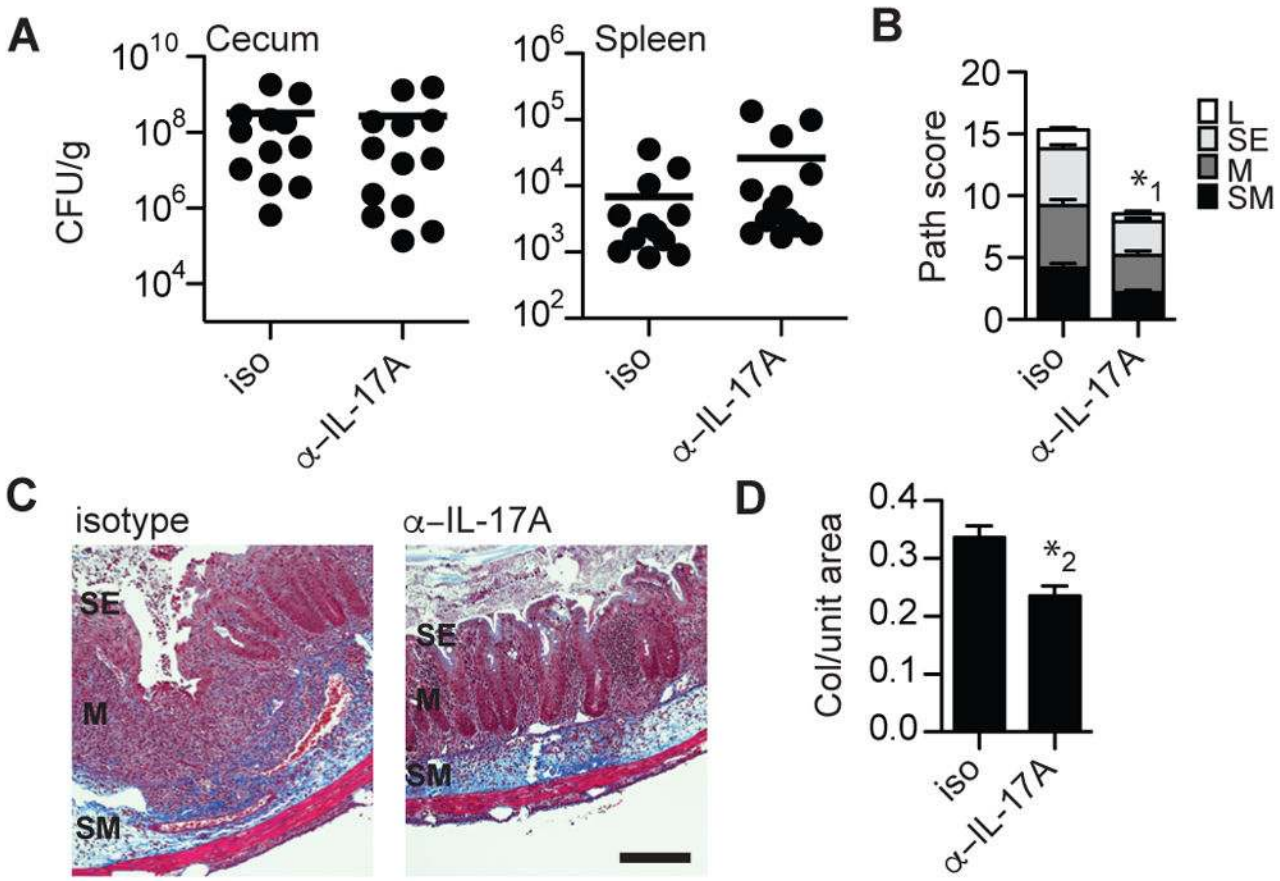

Figure 6. Neutralizing antibodies against IL-17A attenuates fibrosis following *Salmonella* infection

Isotype control (iso) or neutralizing antibodies against IL-17A (α-IL-17A) were administered intraperitoneally to infected mice and sacrificed at day 21. (A) *Salmonella* counts in ceca and spleens. (B–C) Cecal pathology scores and MT-stained tissue sections. L, lumen; SE, surface epithelium; M, mucosa; SM, submucosa. *1, $p=1.10\times10^{-4}$ (n=12, 13 per group, results from two independent experiments). Scale bar, 200 μm. (D) Quantification of submucosal collagen surface area normalized to total tissue surface area. *2, $p=7.80\times10^{-4}$ (n=12, 13 per group, results from two independent experiments). Significance determined by unpaired Student's *t* test.